

NuSTAR J163433–4738.7: A FAST X-RAY TRANSIENT IN THE GALACTIC PLANE

JOHN A. TOMSICK¹, ERIC V. GOTTHELF², FARID RAHOUI^{3,4}, ROBERTO J. ASSEF⁵, FRANZ E. BAUER^{6,7}, ARASH BODAGHEE¹,
STEVEN E. BOGGS¹, FINN E. CHRISTENSEN⁸, WILLIAM W. CRAIG^{1,9}, FRANCESCA M. FORNASINI^{1,10},
JONATHAN GRINDLAY¹¹, CHARLES J. HAILEY², FIONA A. HARRISON¹², ROMAN KRIVONOS¹,
LORENZO NATALUCCI¹³, DANIEL STERN¹⁴, AND WILLIAM W. ZHANG¹⁵

¹ Space Sciences Laboratory, 7 Gauss Way, University of California, Berkeley, CA 94720-7450, USA; jtomsick@ssl.berkeley.edu

² Columbia Astrophysics Laboratory, Columbia University, New York, NY 10027, USA

³ European Southern Observatory, Karl Schwarzschild-Strasse 2, D-85748 Garching bei München, Germany

⁴ Department of Astronomy, Harvard University, 60 Garden Street, Cambridge, MA 02138, USA

⁵ Núcleo de Astronomía de la Facultad de Ingeniería, Universidad Diego Portales, Av. Ejército 441, Santiago, Chile

⁶ Instituto de Astrofísica, Facultad de Física, Pontificia Universidad Católica de Chile, 306, Santiago 22, Chile

⁷ Space Science Institute, 4750 Walnut Street, Suite 205, Boulder, CO 80301, USA

⁸ DTU Space, National Space Institute, Technical University of Denmark, Elektrovej 327, DK-2800 Lyngby, Denmark

⁹ Lawrence Livermore National Laboratory, Livermore, CA 94550, USA

¹⁰ Astronomy Department, University of California, 601 Campbell Hall, Berkeley, CA 94720, USA

¹¹ Harvard-Smithsonian Center for Astrophysics, Cambridge, MA 02138, USA

¹² Cahill Center for Astronomy and Astrophysics, California Institute of Technology, Pasadena, CA 91125, USA

¹³ Istituto Nazionale di Astrofisica, INAF-IAPS, via del Fosso del Cavaliere, I-00133 Roma, Italy

¹⁴ Jet Propulsion Laboratory, California Institute of Technology, Pasadena, CA 91109, USA

¹⁵ NASA Goddard Space Flight Center, Greenbelt, MD 20771, USA

Received 2013 November 6; accepted 2014 February 7; published 2014 March 19

ABSTRACT

During hard X-ray observations of the Norma spiral arm region by the *Nuclear Spectroscopic Telescope Array* (*NuSTAR*) in 2013 February, a new transient source, NuSTAR J163433–4738.7, was detected at a significance level of 8σ in the 3–10 keV bandpass. The source is consistent with having a constant *NuSTAR* count rate over a period of 40 ks and is also detected simultaneously by *Swift* at lower significance. The source is not significantly detected by *NuSTAR*, *Swift*, or *Chandra* in the days before or weeks after the discovery of the transient, indicating that the strong X-ray activity lasted between ~ 0.5 and 1.5 days. Near-infrared imaging observations were carried out before and after the X-ray activity, but we are not able to identify the counterpart. The combined *NuSTAR* and *Swift* energy spectrum is consistent with a power law with a photon index of $\Gamma = 4.1^{+1.5}_{-1.0}$ (90% confidence errors), a blackbody with $kT = 1.2 \pm 0.3$ keV, or a Bremsstrahlung model with $kT = 3.0^{+2.1}_{-1.2}$ keV. The reduced- χ^2 values for the three models are not significantly different, ranging from 1.23 to 1.44 for 8 degrees of freedom. The spectrum is strongly absorbed with $N_{\text{H}} = (2.8^{+2.3}_{-1.4}) \times 10^{23}$ cm⁻², $(9^{+15}) \times 10^{22}$ cm⁻², and $(1.7^{+1.7}_{-0.9}) \times 10^{23}$ cm⁻², for the power-law, blackbody, and Bremsstrahlung models, respectively. Although the high column density could be due to material local to the source, it is consistent with absorption from interstellar material along the line of sight at a distance of 11 kpc, which would indicate an X-ray luminosity $> 10^{34}$ erg s⁻¹. Although we do not reach a definitive determination of the nature of NuSTAR J163433–4738.7, we suggest that it may be an unusually bright active binary or a magnetar.

Key words: Galaxy: stellar content – stars: variables: general – surveys – X-rays: individual (NuSTAR J1634334738.7) – X-rays: stars

Online-only material: color figures

1. INTRODUCTION

Hard X-ray surveys of the Galaxy provide an opportunity to discover populations of extreme sources. The promise of such surveys has been partially realized with the *International Gamma-Ray Astrophysics Laboratory* (*INTEGRAL*; Winkler et al. 2003), which carried out a 20–100 keV survey of the entire Galactic plane and has discovered hundreds of new sources (Bird et al. 2010; Krivonos et al. 2012), including new types of high-mass X-ray binaries (HMXBs), pulsar wind nebulae, and magnetic cataclysmic variables (CVs). The *Nuclear Spectroscopic Telescope Array* (*NuSTAR*; Harrison et al. 2013), which launched in 2012 June and covers the 3–79 keV bandpass, is the first focusing hard X-ray telescope in orbit. While it has a much smaller field of view than *INTEGRAL* does, it has a much lower background and greatly improved sensitivity. Thus, one of *NuSTAR*'s science goals is to extend our view deeper into the Galactic plane to look for hidden hard X-ray populations.

During its first year of operation, *NuSTAR* has initiated surveys of ~ 1 deg² areas both in the Galactic center (e.g., Mori et al. 2013; Nynka et al. 2013) and in a region that samples the spiral arm population in order to probe potentially different environments where X-ray binaries are found. A spiral arm region centered on Galactic coordinates of $l = 337.5$ and $b = 0^\circ$ was chosen for having the highest known density of OB star associations (Russeil 2003) and HMXBs (Bodaghee et al. 2007, 2012). This is part of the Norma spiral arm region, which was identified early in the *INTEGRAL* mission as having an unusually high density of hard X-ray sources (Tomsick et al. 2004; Dean et al. 2005; Lutovinov et al. 2005). The combination of active star formation and evidence that compact objects have already formed suggests that a survey by *NuSTAR* may uncover compact objects associated with populations of massive stars such as magnetars or faint HMXBs that are early in their evolutionary process and may have neutron star or black hole accretors.

Table 1
X-Ray Observations and Count Rates for NuSTAR J163433–4738.7

Mission	Instrument	ObsID	Start Time (UT)	End Time (UT)	Exposure (ks)	Count Rate ^a
Observations in 2011						
<i>Chandra</i>	ACIS-I	12529	Jun 16, 6.97 hr	Jun 16, 12.53 hr	19.0	<0.19
<i>Chandra</i>	ACIS-I	12532	Jun 16, 23.85 hr	Jun 17, 5.55 hr	19.5	<0.21
Observations in 2013						
<i>Swift</i>	XRT	00080509001	Feb 21, 21.70 hr	Feb 21, 23.13 hr	1.79	1.10 ^{+1.77} _{-1.06}
<i>NuSTAR</i>	FPMA	40014004001	Feb 22, 7.77 hr	Feb 22, 17.52 hr	19.4	1.6 ± 0.6
"	FPMB	"	"	"	"	<1.3
<i>Swift</i>	XRT	00080505001	Feb 22, 11.88 hr	Feb 22, 13.71 hr	1.92	<0.54
<i>Swift</i>	XRT	00080506001	Feb 23, 0.83 hr	Feb 23, 2.62 hr	1.98	<1.9
<i>NuSTAR</i>	FPMA	40014007001	Feb 23, 14.52 hr	Feb 24, 1.77 hr	22.6	4.3 ± 0.6
"	FPMB	"	"	"	"	4.4 ± 0.9
<i>Swift</i>	XRT	00080508001	Feb 23, 20.20 hr	Feb 23, 21.70 hr	1.97	2.2 ^{+1.8} _{-1.2}
<i>Swift</i>	XRT	00080511001	Feb 24, 13.72 hr	Feb 24, 15.18 hr	1.75	<0.82
<i>Swift</i>	XRT	00032728001	Feb 28, 1.06 hr	Feb 28, 6.24 hr	4.95	<0.45
<i>Swift</i>	XRT	00032728002	Mar 3, 9.00 hr	Mar 3, 19.06 hr	4.85	<0.12
<i>Swift</i>	XRT	00032728003	Mar 5, 10.66 hr	Mar 5, 20.75 hr	4.47	<1.1
<i>Chandra</i>	ACIS-S	15625	Mar 23, 8.30 hr	Mar 23, 11.91 hr	9.84	<0.50
<i>NuSTAR</i>	FPMA	30001012002	Mar 23, 8.52 hr	Mar 23, 18.35 hr	16.6	<0.50
"	FPMB	"	"	"	"	<2.0

Note. ^a Count rates in the 3–10 keV band in counts per ks. The errors given are 1σ and the upper limits are 90% confidence.

The full surveys of the Galactic Center and the Norma region will be carried out over a period of ~ 2 yr; here, we report on the discovery of a transient source made during the first part of the survey. In this paper, Section 2 describes observations made with *NuSTAR*, *Swift*, and *Chandra*, as well as the procedures we used to reduce the data. The results are presented in Section 3, and we discuss possibilities for the nature of the transient in Section 4.

2. OBSERVATIONS AND DATA REDUCTION

As the first part of the *NuSTAR* survey of the Norma region, nine ~ 20 ks *NuSTAR* observations were performed between UT 2013 February 20 and 24. Each $13' \times 13'$ field of view was partially overlapping with adjacent pointings, and the entire region covered was ~ 0.2 deg². The results from all nine pointings will be reported in Bodaghee et al. (2014). Here, we focus on the observations that covered a new transient, NuSTAR J163433–4738.7. These observations are listed in Table 1, including two that were obtained during the survey and a follow-up *NuSTAR* observation on 2013 March 23 that was coordinated with *Chandra*.

In addition, ~ 2 ks *Swift* X-Ray Telescope observations of the region were carried out during 2013 February 21–24, and four of these observations covered NuSTAR J163433–4738.7. Table 1 lists these along with three other *Swift* observations that were acquired after our survey as part of another observing program. We also analyzed archival data covering the source, including two *Chandra* observations (ObsIDs 12529 and 12532 with exposure times of 19.0 ks and 19.5 ks, respectively) that were acquired in 2011 as part of a survey of the same region being covered by *NuSTAR* (Fornasini et al. 2014).

We reduced the *NuSTAR* and *Swift* data using HEASOFT v6.14 and the latest version of the Calibration Database files as of 2013 August 30. We produced cleaned event lists for the *NuSTAR* focal plane modules A and B (FPMA and FPMB) using nupipeline and for the *Swift* X-Ray Telescope using

xrtpipeline, and further analysis of the event lists is subsequently described. For *Chandra*, we processed the Advanced CCD Imaging Spectrometer (Garmire et al. 2003) data with the *Chandra* Interactive Analysis of Observations software, using chandra_repro to make event lists.

We obtained near-infrared observations covering the NuSTAR J163433–4738.7 error region. This includes *J*, *H*, and *K_s* observations performed on 2011 July 19 with CTIO/NEWFIRM in the framework of near-infrared mapping of the *Chandra* survey field. A detailed description of the data and their reduction can be found in F. Rahoui et al. (in preparation). They were reduced with the dedicated IRAF package NFEXTERN following the standard procedure—tailored for wide-field mosaics—which consists of bad pixel removal, dark subtraction, linearity correction, flatfielding, and median sky subtraction. The resulting images were then flux-calibrated through relative photometry with the 2MASS catalogue. We also obtained *K_s*-band imaging with the Ohio-State Infra-Red Imager/Spectrometer (OSIRIS) at the Southern Astrophysical Research 4.1 m Telescope. We used the f/7 camera, providing a $80''$ field of view, centered at the nominal coordinates of NuSTAR J163433–4738.7. We obtained 36×60 s dithered exposures of the field on 2013 April 3 under good conditions with seeing of $0''.7$, and observed it for 9×60 s again on 2013 April 5, also under good conditions but with somewhat worse seeing of $1''.0$. Reductions were done using the XDIMS IRAF package and photometric calibration was obtained by comparing to 2MASS All-Sky Point Source Catalog sources in the field.

3. RESULTS

The new transient was discovered from an inspection of the image from the 22.6 ks *NuSTAR* observation that took place starting on 2013 February 23, 14.52 hr. As shown in Figure 1, the source was detected in FPMA and FPMB. To determine the significance of the detection, we extracted 3–10 keV counts from a $30''$ radius circle centered on the approximate position

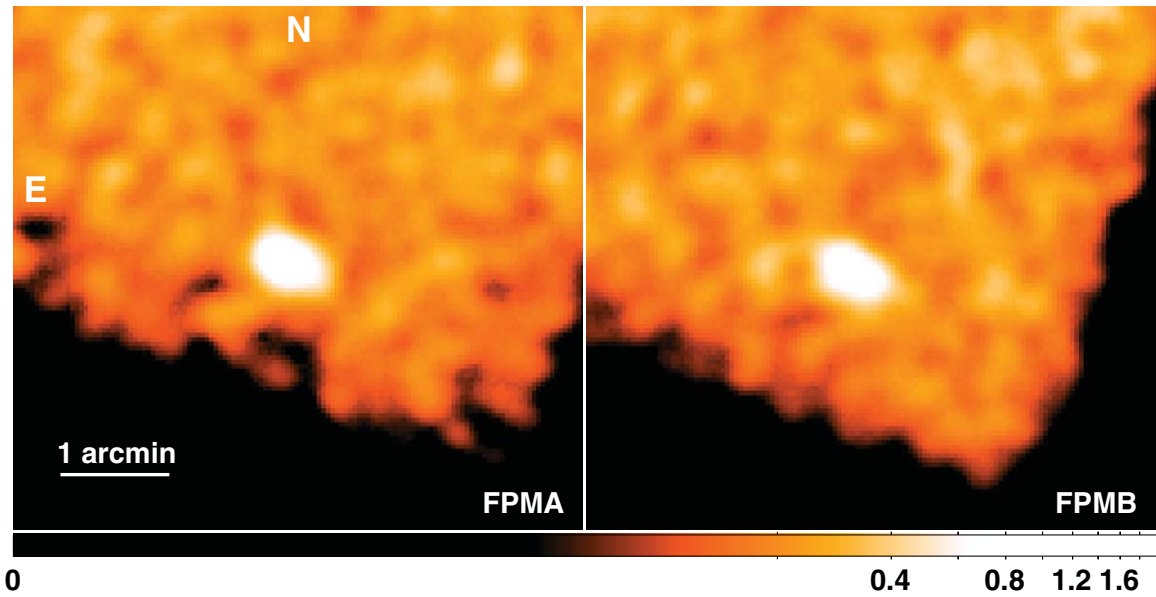


Figure 1. *NuSTAR* discovery images in the 3–20 keV energy band for NuSTAR J163433–4738.7. The source was detected in both of the *NuSTAR* focal plane modules A and B in a 22.6 ks exposure taken on 2013 February 23–24. The images have been rebinned so that the pixel size is $2''.5$ and smoothed with a 6 pixel Gaussian. The scale on the bottom of the figure is in counts per pixel, and a logarithmic scaling is used. The apparent elongation of the source is due to the distorted point spread function shape at large off-axis angles.

(A color version of this figure is available in the online journal.)

of the source. We determined the background level using a nearby source-free circular region with a radius of $90''$. After background subtraction, we obtained 97 ± 14 and 99 ± 20 counts in FPMA and FPMB, respectively. The combined significance is 8.0σ , confirming the detection.

To determine the source position, we extracted all of the events from a $60'' \times 60''$ square region and made histograms of the counts, binning in the R.A. and decl. directions. We performed χ^2 fitting of the histograms with a model consisting of a constant (accounting for the flat background) and a Gaussian for the source. It should be noted that this is an approximation since the *NuSTAR* point spread function is non-Gaussian. We determined the centroids separately for FPMA and FPMB, and they are consistent with each other. The weighted average of the two centroids is R.A. = $16^{\text{h}}34^{\text{m}}33^{\text{s}}.42$, decl. = $-47^{\circ}38'41''.9$ (J2000.0) with 3σ statistical uncertainties of $6''.3$ and $4''.9$ in R.A. and decl., respectively. After considering that the systematic pointing uncertainty for *NuSTAR* is $\sim 8''$ (Harrison et al. 2013), the error region can be approximated with a $10''$ radius circle.

We searched online catalogs (e.g., SIMBAD¹⁶) for X-ray sources consistent with the position of NuSTAR J163433–4738.7, but we did not find any likely candidates. The catalog from the 2011 *Chandra* survey (F. M. Fornasini et al., submitted) does not have any sources in the NuSTAR J163433–4738.7 error region. On the basis of this and the analysis subsequently described (including a reanalysis of the 2011 *Chandra* observations), we conclude that NuSTAR J163433–4738.7 is a previously undetected source and that it is very likely to be a transient given the sensitivity of the *Chandra* observations.

For the *NuSTAR* and *Swift* observations listed in Table 1, we estimated count rates or upper limits for NuSTAR J163433–4738.7 using $30''$ radius source regions centered at the source position derived from ObsID 40014007001. The X-Ray Telescope 90% encircled energy radius is approximately

$20''$, but we use $30''$ to account for the uncertainty in the source position as NuSTAR J163433–4738.7 is not bright enough in any of the *Swift* observations to improve the measurement of the source position. As described earlier, we used a larger, circular region that does not contain any detected point sources for background. Selecting the background regions for *NuSTAR* requires some care because of scattered light from a nearby bright source (4U 1630–47).

The 3–10 keV count rates or limits obtained for all observations are given in Table 1. For *NuSTAR*, the background rates are high enough to use Gaussian statistics, and we use the Poisson limits tabulated in Gehrels (1986) for *Swift* and *Chandra*. In all cases, we quote the 1σ error bars if the minimum of the 1σ error region is positive. Otherwise, we give the 90% confidence upper limit. While the *NuSTAR* observation taken on February 23 provides the only highly significant detection, the *Swift* observation with the highest count rate is the one that occurred during this *NuSTAR* observation. The only other possible evidence for activity from NuSTAR J163433–4738.7 occurred on February 22, when *NuSTAR* obtained a 2.7σ detection in focal plane module B data.

For *Chandra* ObsIDs 12529 and 12532 (from 2011) and ObsID 15625 (from 2013), we analyzed the Advanced CCD Imaging Spectrometer data to search for a detection of NuSTAR J163433–4738.7. On the basis of an inspection, no sources are apparent in the 0.3–10 keV or 3–10 keV images. The source is $7'$ and $5'$ from the *Chandra* aimpoint for the 2011 ObsIDs. At these off-axis angles, the 90% encircled energy fraction (EEF) radii (for 4.5 keV photons) are $7''.4$ and $4''.5$ for ObsIDs 12529 and 12532, respectively. ObsID 15625 was a dedicated pointing with the target on-axis, and the 90% EEF radius is $2''$. For ObsID 12529, the largest number of 3–10 keV counts within any $7''.4$ radius circle inside the *NuSTAR* error region is three, and, after accounting for background, we calculate a 90% confidence upper limit of $< 1.9 \times 10^{-4} \text{ s}^{-1}$ on the count rate (see Table 1).

¹⁶ <http://simbad.u-strasbg.fr/simbad>

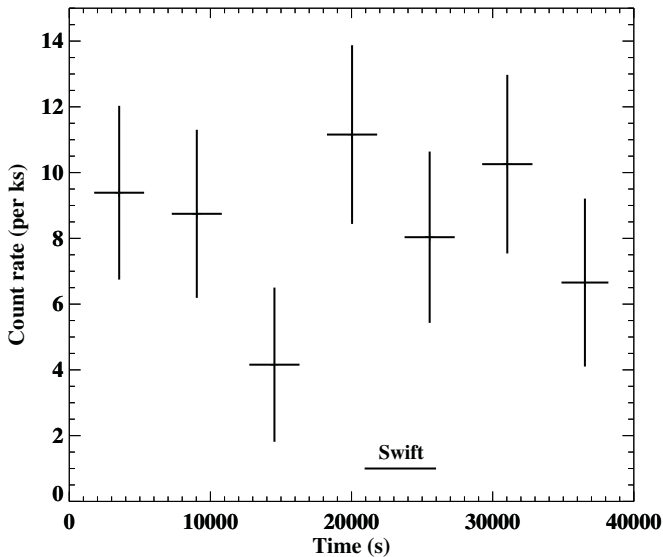


Figure 2. 3–10 keV *NuSTAR* light curves (focal plane modules A and B after background subtraction) for NuSTAR J163433–4738.7 during ObsID 40014007001. There is one data point per satellite orbit. The errors on the data points are at 1σ confidence. The time of a *Swift* observation is indicated. Zero on the time axis corresponds to MJD 56,346.60000.

For ObsID 12532, the largest number of 3–10 keV counts within any $4/5$ radius circle inside the *NuSTAR* error region is two, and the count rate limit is $<2.1 \times 10^{-4} \text{ s}^{-1}$. For ObsID 15625, the largest number of 3–10 keV counts within a $2''$ radius circle is two, and the count rate limit is $<5.0 \times 10^{-4} \text{ s}^{-1}$. This is higher than for the 2011 ObsIDs because of the lower exposure time.

We made *NuSTAR* light curves for ObsID 40014007001 with several different time binnings between 0.1 s and 5500 s (the approximate satellite orbital period) in the 3–10 keV and 3–79 keV bandpasses. The lack of any apparent variability in the 0.1–10 s light curves rules out flares or bursts that might prove the presence of a neutron star. Figure 2 shows the 3–10 keV orbit-by-orbit light curve for FPMA and FPMB combined. At the 5500 s binning, a χ^2 test shows that the 3–10 keV and 3–79 keV light curves are consistent with the source being constant over ~ 40 ks.

Next, we extracted *NuSTAR* FPMA and FPMB spectra for ObsID 40014007001 and an X-Ray Telescope spectrum for ObsID 00080508001, which are the two observations with significant detections of NuSTAR J163433–4738.7. These were fitted jointly by minimizing the Cash (or C) statistic (Cash 1979) using the XSPEC software package. The statistical quality of the spectrum is low, and it is well fit by a power-law, a blackbody, or a thermal Bremsstrahlung model. In all three cases, we included absorption using Wilms et al. (2000) abundances and Verner et al. (1996) cross-sections. The parameters are given in Table 2, and the errors quoted are 90% confidence for one parameter of interest, $\Delta C = 2.7$. Although we used the C -statistic to determine the parameters, we also calculated the reduced- χ^2 values, and they appear in Table 2. This quantity is slightly smaller for the power-law model ($\chi^2_{\nu} = 1.23$ for 8 degrees of freedom) compared with the blackbody model ($\chi^2_{\nu} = 1.44$ for 8 dof) and the Bremsstrahlung model ($\chi^2_{\nu} = 1.29$ for 8 dof). However, given the small number of dof, the difference in χ^2_{ν} is not significant, and the steeply falling power-law index ($\Gamma = 4.1^{+1.5}_{-1.0}$) suggests that the emission probably has a thermal origin. The spectrum for the blackbody model is shown in Figure 3.

Table 2
Parameters for Fits to *NuSTAR* and *Swift* X-Ray Telescope Spectra

Model	N_{H}^{a}	Γ or kT	Flux ^b	C-statistic ^c	χ^2_{ν}/dof
Power-law	28^{+23}_{-14} d	$4.1^{+1.5}_{-1.0}$	4^{+18}_{-2}	9.5	1.23/8
Blackbody	9^{+15}_{-7}	$1.2 \pm 0.3 \text{ keV}$	$1.0^{+0.8}_{-0.3}$	11.2	1.44/8
Bremsstrahlung	17^{+17}_{-9}	$3.0^{+2.1}_{-1.2}$	$1.6^{+2.0}_{-0.6}$	9.8	1.29/8

Notes.

^a The column density in units of 10^{22} cm^{-2} .

^b The 2–10 keV unabsorbed flux in units of $10^{-12} \text{ erg cm}^{-2} \text{ s}^{-1}$

^c We fitted the spectra by minimizing the Cash statistic.

^d All errors in this table are quoted at the 90% confidence level.

We used the absorbed blackbody model and the count rates for *NuSTAR*, *Swift*, and *Chandra* given in Table 1 to calculate measurements or upper limits on the absorbed 3–10 keV flux, and these flux histories are shown in Figure 4. We also calculated the flux upper limits for the *Chandra* observations from 2011. The upper limits on the absorbed 3–10 keV fluxes are $<1.6 \times 10^{-14} \text{ erg cm}^{-2} \text{ s}^{-1}$ and $<2.5 \times 10^{-14} \text{ erg cm}^{-2} \text{ s}^{-1}$ for ObsIDs 12529 and 12532, respectively. Although the count rate limits are considerably lower for these ObsIDs compared with *Chandra* ObsID 15625, the flux limits are similar because of the different effective areas for the ACIS-I and ACIS-S instruments. The lowest *Chandra* upper limit indicates that the flux from this source changed by at least a factor of 39^{+6}_{-4} , suggesting that it is a transient rather than simply being a highly variable X-ray source.

The *NuSTAR* error circle includes dozens of near-infrared candidate counterparts brighter than $K_s \sim 17$ (Vega magnitude system). In the NEWFIRM images from 2011, the brightest source in the error circle (2MASS J16343288–4738393) has $K_s = 12.33 \pm 0.05$, $H = 13.07 \pm 0.06$, and $J = 14.61 \pm 0.05$, and the 2MASS magnitudes are consistent, indicating a possible lack of variability on long timescales. The next two brightest sources are 2MASS J16343362–4738479 at $K_s = 13.31 \pm 0.05$ and the *Spitzer*/GLIMPSE source G336.7870+00.0111 at $K_s = 14.70 \pm 0.05$. These may be more likely counterparts to NuSTAR J163433–4738.7 because they are relatively highly reddened ($H - K_s = 2.35 \pm 0.08$ and 1.34 ± 0.08 , respectively). However, we do not find any evidence that these sources are variable. For the two OSIRIS K_s images taken on April 3 and April 5, we performed aperture photometry for all of the sources within the *NuSTAR* error circle, but did not find any variable sources.

The high time-resolution of the *NuSTAR* data allows for a search for a coherent signal with periods $P \geq 4$ ms, covering the range expected for either an isolated rotation-powered pulsar, a binary, or a magnetar. Given the paucity of source counts in the observations listed in Table 1, we concentrate our attention on the ObsID 40014007001 data. Photon arrival times, adjusted for the *NuSTAR* clock drift, were corrected to the Solar System barycenter using JPL DE200 ephemeris and the *NuSTAR* derived source coordinates. We extracted photons in the 3–10 keV band from a $30''$ radius aperture centered on the source to optimize the signal-to-noise ratio. We searched for significant power from a coherent signal using an fast Fourier transform (FFT) sampled at the Nyquist frequency. The observation span was too short to consider the smearing of the pulse profile by spin-down of even the most highly energetic pulsar or the typical binary orbit period. The most significant signal found has a power of $P = 35.18$, corresponding to a probability of false detection

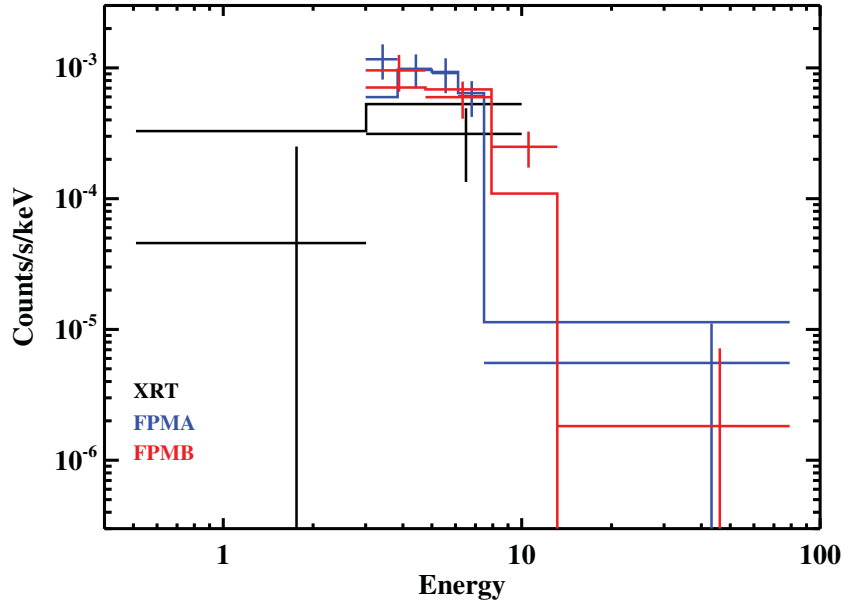


Figure 3. *NuSTAR* and *Swift* energy spectra for NuSTAR J163433–4738.7 on 2013 February 23–24 fitted with an absorbed blackbody model. The black, blue, and red data points and model lines correspond to the X-Ray Telescope, focal plane module A, and focal plane module B, respectively. The errors on the data points are 1σ confidence.

(A color version of this figure is available in the online journal.)

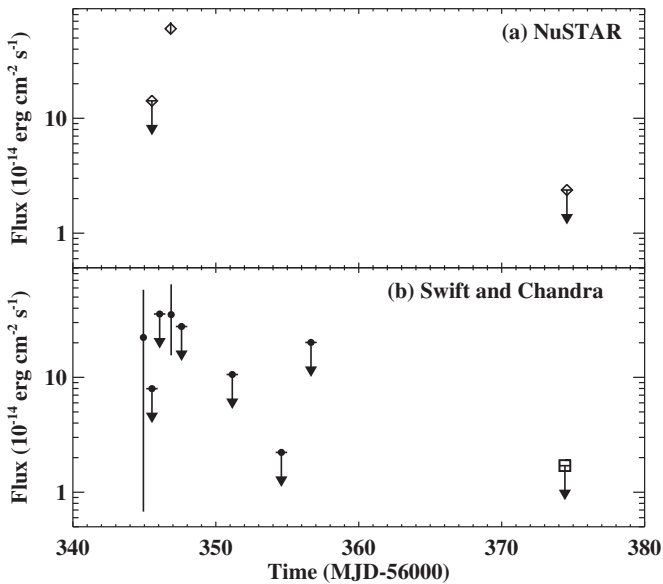


Figure 4. *NuSTAR*, *Swift*, and *Chandra* (marked with diamonds, filled circles, and a square, respectively) absorbed 3–10 keV fluxes for NuSTAR J163433–4738.7 assuming an absorbed blackbody with a column density of $N_{\text{H}} = 9 \times 10^{22} \text{ cm}^{-2}$ and a temperature of 1.2 keV. The errors on the data points are 1σ significance, and the upper limits are 90% confidence.

of $\varphi = 0.8$ for 2^{25} FFT search trials. We conclude that no pulsed X-ray signal is detected in from NuSTAR J163433–4738.7. After taking into account the local background, we place an upper limit on the pulse fraction at the 3σ confidence level of $f_p < 36\%$ for a blind search for a sinusoidal signal $P > 4$ ms.

4. DISCUSSION

In considering the nature of NuSTAR J163433–4738.7, it is useful to estimate the X-ray luminosity that the source reached during its outburst. Although the distance is highly uncertain, the strong absorption indicates either a large distance through

a region of the Galaxy with heavy extinction or absorption local to the source. The former is a strong possibility because the transient is in the direction of a region of the Galactic plane that is crowded with H II/molecular cloud regions. NuSTAR J163433–4738.7 is at $l = 336^\circ 787$, $b = +0^\circ 014$, near a group of H II regions (336.732 ± 0.072 , 336.840 ± 0.047 , 336.9 ± 0.1 , 337.147 ± 0.181 , and 337.3 ± 0.1) at a distance of 10.9 ± 0.2 kpc (Georgelin et al. 1996; Russeil 2003).¹⁷ If the absorption is interstellar, then NuSTAR J163433–4738.7 is very likely beyond or in these molecular clouds, indicating a 2–10 keV unabsorbed luminosity limit of $>9 \times 10^{33} \text{ erg s}^{-1}$ for Bremsstrahlung. In the following, we consider both possibilities: a distance of ~ 11 kpc and a peak luminosity of $\sim 10^{34} \text{ erg s}^{-1}$; and a smaller distance with absorption local to the source and a lower luminosity.

Considering the first possibility, a luminosity as high as $10^{34} \text{ erg s}^{-1}$ would be unprecedented for at least two common types of X-ray sources in the Galaxy. Nonmagnetic CVs have strong optical outbursts along with persistent and transient X-ray emission. However, extensive studies have shown that their X-ray luminosities are in the $10^{29-32} \text{ erg s}^{-1}$ range (Baskill et al. 2005; Kuulkers et al. 2006). While magnetic CVs can reach higher luminosities (Kuulkers et al. 2006), they do not typically show outbursts. Second, active binaries, including RS CVn systems and low-mass flare stars, produce X-ray flares, some of which can last for about a day. Superflares that peak at X-ray luminosities of $10^{32-33} \text{ erg s}^{-1}$ have been seen (Francosini et al. 2001; Osten et al. 2007, 2010; Pandey & Singh 2012), and there have been flares that have released $\gtrsim 10^{37} \text{ erg}$ (Francosini et al. 2001). If NuSTAR J163433–4738.7 is at ~ 11 kpc, then in addition to having a higher peak luminosity, the energy released is $\gtrsim 4 \times 10^{38} \text{ erg}$, which is based on the source being at its peak luminosity for $\gtrsim 40$ ks (see Figure 2).

¹⁷ This kinematic distance is estimated using the mean Galactic rotation curve, and the uncertainty does not account for possible deviations relative to the mean.

In summary, while we do not rule out the active binary possibility (and see later in this paper further discussion on this topic), at the 11 kpc distance, the event seen by *NuSTAR* would need to be extreme for this explanation to be correct.

A source type that might be a good match to the *NuSTAR* J163433–4738.7 properties is the class of highly magnetic isolated neutron stars: magnetars. While these sources are best known for their very bright and brief (~ 0.1 s) X-ray and gamma-ray flares, they also have persistent but variable emission that can easily reach 10^{34} erg s $^{-1}$ or higher (Woods & Thompson 2006). The X-ray spectrum of their persistent emission is dominated by a ~ 0.5 –1 keV blackbody (Woods & Thompson 2006; Mori et al. 2013). Furthermore, as mentioned in Section 1, magnetars are associated with regions where high-mass star formation is occurring, such as the Norma region, and there is a known magnetar, SGR 1627–41, that is ~ 0.2 from *NuSTAR* J163433–4738.7. However, one possible counterargument to the magnetar hypothesis is that magnetar periods of activity usually last for months. From Figure 4, the peak activity from *NuSTAR* J163433–4738.7 could not have lasted for more than ~ 1.5 days based on the *Swift* upper limits, and *Chandra* and *NuSTAR* place a tight upper limit on activity ~ 3 weeks after the *NuSTAR* detection. While we do not detect pulsations or ~ 0.1 s flares, which would prove that the source is a magnetar, the pulsation search is limited by the statistical quality of the data, and flaring episodes are relatively rare.

A blackbody spectrum could also be produced from an optically thick accretion disk in a black hole binary. Most often, such sources show temperatures of ~ 1 keV in the inner parts of their accretion disks when they are at high luminosity $\gtrsim 10^{36-37}$ erg s $^{-1}$, which would require a very large distance of $\gtrsim 100$ –300 kpc for *NuSTAR* J163433–4738.7. Two sources (GRS 1758–258 and 1E 1740.7–2942) have shown fainter soft states, but their blackbody spectra have been at temperatures of 0.4 keV (Smith et al. 2001) and 0.7 keV (del Santo et al. 2005), which are lower than the 1.2 keV we see for *NuSTAR* J163433–4738.7. Also, transient black hole binaries typically have outbursts that last for several months, which is very different from *NuSTAR* J163433–4738.7.

Considering the second possibility that the source is closer than ~ 11 kpc, then the high column density must be due to material local to the source. *INTEGRAL* has found a large number of obscured HMXBs that have column densities of 10^{23-24} cm $^{-2}$ due to the wind from their supergiant companions (e.g., Walter et al. 2006). While many of the sources in this class are persistent, the supergiant fast X-ray transients (SFXTs), which have some members that are also obscured HMXBs, have outbursts that can be as short as a few hours, and it would not be unusual for an SFXT to produce X-ray emission that lasts for half a day (Smith et al. 1998; Negueruela et al. 2006; Romano et al. 2011). However, a possible problem for this interpretation is that the spectrum of *NuSTAR* J163433–4738.7 is softer than usually seen for active SFXTs. During flares, IGR J17544–2619 and IGR J16479–4514 show a power-law spectrum with a photon index near $\Gamma = 1.4$ (Rampy et al. 2009; Sidoli et al. 2013). Somewhat softer spectra with $\Gamma \sim 2.3$ –2.4 can be seen during periods of weaker activity, but their spectra are only as soft as *NuSTAR* J163433–4738.7 when they are in quiescence.

For CVs and active binaries, the challenge is to explain a column density as high as we measure with absorption local to the systems. One possibility is that material expelled from the system (either related to the evolutionary state of the stellar component or related to the X-ray flaring event)

could cause increased column density. However, for one active binary (AX Ari), the column density was seen to increase to $N_{\text{H}} = 1.1 \times 10^{20}$ cm $^{-2}$ during an event (Franciosi et al. 2001), which is two to three orders of magnitude less than is required for *NuSTAR* J163433–4738.7. Variation in optical brightness of some stars has also been attributed to the ejection of material from the stars. An example of this is a change of 0.5 mag in the optical seen for KU Cyg (Tang et al. 2011). However, this would translate into a column density near 10^{21} cm $^{-2}$, which is still far less than is required.

The near-infrared information that we have provides only weak constraints on the source type. Given that we were not able to identify the counterpart, we can only say that the source must be fainter (before and after the X-ray flare) than the brightest source in the error circle (2MASS J16343288–4738393). This corresponds to $K_s > 12.3$, $H > 13.1$, and $J > 14.6$, and these values are consistent with all of the possibilities for the source type discussed above. However, in the scenario where *NuSTAR* J163433–4738.7 is a nearby source with local absorption, these limits do provide some constraint. For example, a very nearby and luminous obscured HMXB is ruled out.

In summary, *NuSTAR* J163433–4738.7 is a fast X-ray transient that has a thermal spectrum with relatively high temperature ($kT = 1.2$ keV for a blackbody or 3.0 keV for Bremsstrahlung). If its high column density is due to interstellar material, the source is probably distant ($\gtrsim 11$ kpc), making the peak luminosity $\gtrsim 10^{34}$ erg s $^{-1}$. We discuss the origin of the flare and suggest that the most likely possibilities if the source is distant are an unusually bright flare from an active binary or a short outburst from a magnetar. We also consider the possibility that the source is closer and that the absorption is local to the source. More *NuSTAR* observations in the Galactic plane will determine whether such transients are common and, hopefully, shed light on the nature of *NuSTAR* J163433–4738.7.

This work was supported under NASA Contract No. NNG08FD60C, and made use of data from the *NuSTAR* mission, a project led by the California Institute of Technology, managed by the Jet Propulsion Laboratory, and funded by the National Aeronautics and Space Administration. The authors thank the *NuSTAR* Operations, Software, and Calibration teams for support with the execution and analysis of these observations. This research has made use of the *NuSTAR* Data Analysis Software (*NuSTARDAS*) jointly developed by the ASI Science Data Center (Italy) and the California Institute of Technology (USA). R.J.A. was supported by Gemini-CONICYT grant 32120009. F.E.B. was supported by Basal-CATA PFB-06/2007 and CONICYT-Chile (through FONDECYT 1101024, Gemini-CONICYT 32120003, and Anillo ACT1101). L.N. wishes to acknowledge the Italian Space Agency (ASI) for financial support by ASI/INAF grant I/037/12/0-011/13. The authors thank Harvey Tananbaum for providing *Chandra* Director’s Discretionary Time for this project. This research has made use of the SIMBAD database, operated at CDS, Strasbourg, France.

REFERENCES

- Baskill, D. S., Wheatley, P. J., & Osborne, J. P. 2005, *MNRAS*, 357, 626
 Bird, A. J., Bazzano, A., Bassani, L., et al. 2010, *ApJS*, 186, 1
 Bodaghee, A., Courvoisier, T. J.-L., Rodriguez, J., et al. 2007, *A&A*, 467, 585
 Bodaghee, A., Tomsick, J. A., Krivonos, R., et al. 2014, *ApJ*, submitted
 Bodaghee, A., Tomsick, J. A., Rodriguez, J., & James, J. B. 2012, *ApJ*, 744, 108

- Cash, W. 1979, *ApJ*, **228**, 939
- Dean, A. J., Bazzano, A., Hill, A. B., et al. 2005, *A&A*, **443**, 485
- del Santo, M., Bazzano, A., Zdziarski, A. A., et al. 2005, *A&A*, **433**, 613
- Fornasini, F. M., Tomsick, J. A., Bodaghee, A., et al. 2014, *ApJ*, submitted
- Franciosini, E., Pallavicini, R., & Tagliaferri, G. 2001, *A&A*, **375**, 196
- Garmire, G. P., Bautz, M. W., Ford, P. G., Nousek, J. A., & Ricker, G. R. 2003, *Proc. SPIE*, **4851**, 28
- Gehrels, N. 1986, *ApJ*, **303**, 336
- Georgelin, Y. M., Russeil, D., Marcelin, M., et al. 1996, *A&AS*, **120**, 41
- Harrison, F. A., Craig, W. W., Christensen, F. E., et al. 2013, *ApJL*, **770**, 103
- Krivonos, R., Tsygankov, S., Lutovinov, A., et al. 2012, *A&A*, **545**, A27
- Kuulkers, E., Norton, A., Schwope, A., & Warner, B. 2006, in *Compact stellar X-ray Sources*, ed. W. Lewin & M. van der Klis (Cambridge: Cambridge Univ. Press), 421
- Lutovinov, A., Revnivtsev, M., Gilfanov, M., et al. 2005, *A&A*, **444**, 821
- Mori, K., Gotthelf, E. V., Zhang, S., et al. 2013, *ApJL*, **770**, L23
- Negueruela, I., Smith, D. M., Reig, P., Chaty, S., & Torrejón, J. M. 2006, in *The X-ray Universe 2005*, ed. A. Wilson (ESA SP-604; Noordwijk: ESA), 165
- Nynka, M., Hailey, C. J., Mori, K., et al. 2013, *ApJL*, **778**, L31
- Osten, R. A., Drake, S., Tueller, J., et al. 2007, *ApJ*, **654**, 1052
- Osten, R. A., Godet, O., Drake, S., et al. 2010, *ApJ*, **721**, 785
- Pandey, J. C., & Singh, K. P. 2012, *MNRAS*, **419**, 1219
- Rampy, R. A., Smith, D. M., & Negueruela, I. 2009, *ApJ*, **707**, 243
- Romano, P., La Parola, V., Vercellone, S., et al. 2011, *MNRAS*, **410**, 1825
- Russeil, D. 2003, *A&A*, **397**, 133
- Sidoli, L., Esposito, P., Sguera, V., et al. 2013, *MNRAS*, **429**, 2763
- Smith, D. M., Heindl, W. A., Markwardt, C. B., & Swank, J. H. 2001, *ApJL*, **554**, L41
- Smith, D. M., Main, D., Marshall, F., et al. 1998, *ApJL*, **501**, L181
- Tang, S., Grindlay, J., Los, E., & Servillat, M. 2011, *ApJ*, **738**, 7
- Tomsick, J. A., Lingenfelter, R., Corbel, S., Goldwurm, A., & Kaaret, P. 2004, in *5th INTEGRAL Workshop on the INTEGRAL Universe* (Noordwijk: ESA), 413
- Verner, D. A., Ferland, G. J., Korista, K. T., & Yakovlev, D. G. 1996, *ApJ*, **465**, 487
- Walter, R., Zurita Heras, J., Bassani, L., et al. 2006, *A&A*, **453**, 133
- Wilms, J., Allen, A., & McCray, R. 2000, *ApJ*, **542**, 914
- Winkler, C., Courvoisier, T. J. L., Di Cocco, G., et al. 2003, *A&A*, **411**, L1
- Woods, P. M., & Thompson, C. 2006, in *Compact Stellar X-ray Sources*, ed. W. Lewin & M. van der Klis (Cambridge: Cambridge Univ. Press), 547